EXPERIMENTS WITH DOUBLE MICROWAVE APERTURES

John P. Basart and Zhong Zhang
Center for Nondestructive Evaluation and
Department of Electrical and Computer Engineering
Iowa State University
Ames, IA 50011

One of the significant characterizations of microwave imaging is the spatial resolution. The relative long wavelength of microwaves as compared to ultrasonic waves and x-rays necessarily means that aperture arrays (real-time or synthetic) are required for high-resolution microwave imaging. Certain limitations on resolution apply regardless of how the array is realized. Types of antenna arrays fall into two broad categories: Phased arrays which are usually operated in real time by scanning a beam past an object, and aperture synthesis in which data are collected with one or more antennas and later processed to produce an image. In NDE we are concerned with the linear resolution which we define as the product of the angular resolution and the range from the array phase center to the object of interest. For objects imaged in the far field of the array, the angular resolution is inversely proportional to the largest size of the array. We have conducted a series of experiments to study the practical and mathematical aspects of resolution when the object of interest is physically near the microwave apertures.

The resolution of an array is principally determined by the largest dimension of the array in terms of wavelength, so experiments done with two horns provide resolution information representative of an entire array. The purpose of our experiments was to study resolution obtained when scanning an object from one side, which we are often limited to in NDE.

There are several tradeoffs to consider when scanning an object with microwaves. Increasing the aperture size improves the resolution, but also increases the onset of the far field which may alter an experiment. However, with appropriate data analysis one can do near-field imaging. The angular resolution of an array can be increased by increasing the array size, but this can lead to physically large arrays that could be unwieldy. To increase linear resolution we can increase angular resolution and/or decrease the range. Decreasing the range often can be the easiest thing to do, but it can create difficulties. For instance, the resolution will change as a beam scans over an object because the effective antenna separation, when projected in the direction of the target, changes. The closer the array is to the object, the greater the change in resolution across the object as the beam is scanned.

There are also tradeoffs in the two types of arrays: phased and synthetic. The principal advantage of a phased array is that it produces a real-time beam. With rapid electronic scanning, images can be made quickly by raster scanning which decreases inspection time and allows the inspector to quickly try various laboratory configurations. A disadvantage of the phased array is that it requires a lot of hardware and a complex interconnection of many antenna elements. It also requires a moderately elaborate software package for controlling the array.

Review of Progress in Quantitative Nondestructive Evaluation, Vol. 12
Edited by D.O. Thompson and D.E. Chimenti, Plenum Press, New York, 1993

The advantages and disadvantages of a synthetic aperture are basically the opposite of the phased array. The beam does not occur in real time, but is synthesized by one or more antennas mechanically moved to gather the information. Amplitudes and phases from all scans must be accurately measured and combined to produce an image. Because of combining amplitudes and phases after the fact, we have the advantage of being able to control the beam that is synthesized. By appropriately altering the amplitudes and phases, various types of beams can be produced. This allows us to make tradeoffs between beamwidth and sidelobe level off line. The data can be repeatedly analyzed with different adjustment factors to produce an optimum image for the information to be gathered. With these various tradeoffs, it is appropriate to try to match the array to the type of information to be obtained.

Our experiments were conducted with the equipment shown schematically in Fig. 1. The transmitter chain consists of the usual equipment with frequency and power measuring equipment. The receiving equipment consisted of two antennas on equal length arms connected to a detector and signal recording equipment. The experiments were conducted by choosing a range distance between the transmitting and receiving antennas, and then rotating the turntable with the receiving antennas over a limited angle. The resulting power patterns are shown in Figs. 2 and 3. The figures plot normalized intensity (power units) vs. scanning angle of the turntable.

In Fig. 2 (left) with a range of 183 cm and a receiving antenna separation of 54 cm, the main features are a fringe pattern whose amplitude is determined by the power pattern of the individual receiving horns which were identical. The width of the fringe pattern is inversely proportional to the separation between the receiving antennas. The separation between minima adjacent to the main lobe is given in radians by λ/D where λ is the wavelength and D is the separation between the phase centers of the horns in the receiving array. Notice that the minima in Fig. 2 (left) are lifted above zero to the left and right of center. This is caused by a near-field phenomenon for arrays. There is a noticeable change in the range to the left (right) antenna as the turntable rotates counterclockwise (clockwise). The signal is measurably stronger in the left (right) antenna than in the right (left) antenna. This unbalance in the amplitude of the two signals received at the detector prevents the nulls from dropping to zero when the two signals are 180 degrees out of phase.

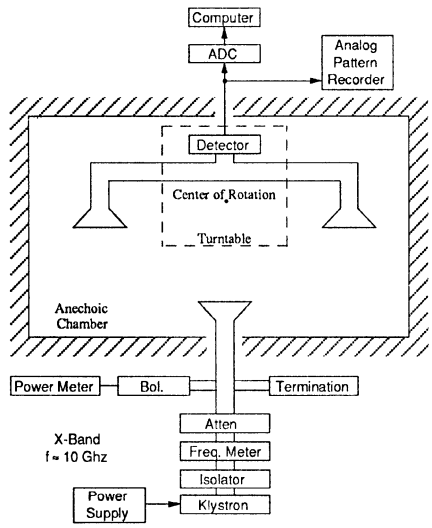

Fig. 1. Experimental set-up.

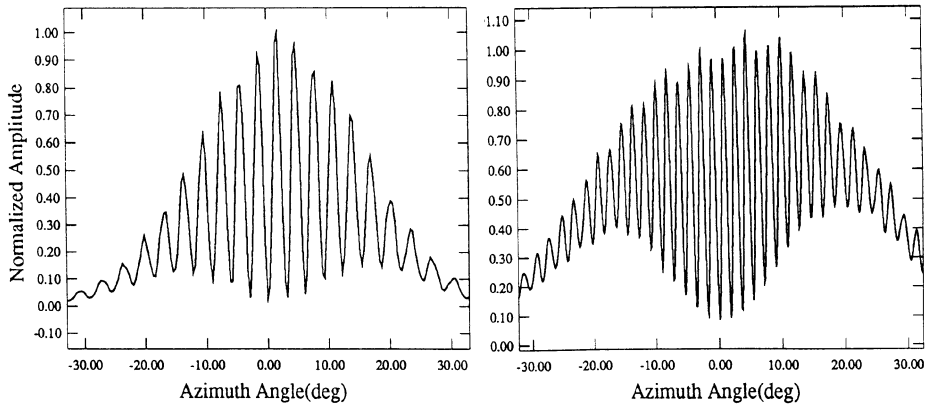

Fig. 2. Experimental fringe pattern with a range of 183 cm and a receiving antenna separation of 54 cm (left) and a separation of 94 cm (right).

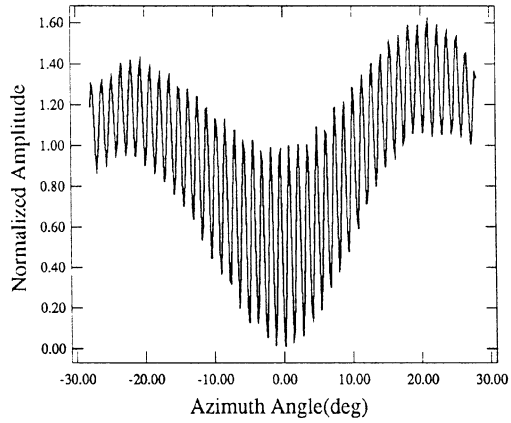

Fig. 3. Experimental fringe pattern with a range of 183 cm and a receiving antenna separation of 132 cm.

In Fig. 2 (right) the antenna separation, D, was increased to 94 cm. The upper envelope has widened and the nulls on either side of center have risen considerably. The fringe width has expectedly narrowed. Continuing to widen the antenna separation to 132 cm, we see in Fig. 3 a gross change in the pattern compared to the patterns in Fig. 2. In addition to the extreme lifting of the nulls, the peak of the upper envelope has now divided into two lobes. These changes are due to the same effect that has been described. In many applications these phenomena are not observed because the range is very large compared to the antenna separation.

We can explain the pattern behavior with relatively simple mathematics. The symbols used are defined in Fig. 4. Angle θ is the rotation angle of the pair of antennas while ϕ_1 and ϕ_2 are the pattern angles for the individual antennas in their own reference frame. R_1 and R_2 are the ranges from the transmitting antenna to the phase centers of the respective receiving antennas. Since the individual receiving antennas are essentially in the far field

of the transmitting antenna we can use far-field mathematics for the signal to each receiving antenna. The transmitting antenna pattern is sufficiently broad that its pattern is neglected. The expression for the fringe pattern coming out of the receiver is given by

$$f_r = p(\phi_1)\frac{e^{-j2\pi R_1/\lambda}}{R_1} + p(\phi_2)\frac{e^{-j2\pi R_2/\lambda}}{R_2} \tag{1}$$

where $p(\phi_1)$ and $p(\phi_2)$ are the amplitude (voltage) patterns of antennas one and two, respectively. In our situation the patterns of the two receiving horns are the same, but ϕ_1 and ϕ_2 are not equal angles since we do much of our calculations in the near field of the array.

To verify that this expression basically explains the measured patterns, we calculated the power patterns using the range and antenna separations of the measured patterns (Figs. 2 and 3). The results are shown in Figs. 5 and 6 where θ is plotted on the abcissa. We can see that the theoretical results basically agree with the experimental results (compare Figs. 2 and 5, and 3 and 6). The differences are due to the small amplitude and phase effects not accounted for in the actual hardware. The disturbances in the array pattern are due to the near field effects of the *array*, but we are using the mathematics of the far field of the antenna elements. The significance of the agreement between equation (1) and the measurements is that we can use equation (1) in describing the resolution of the array.

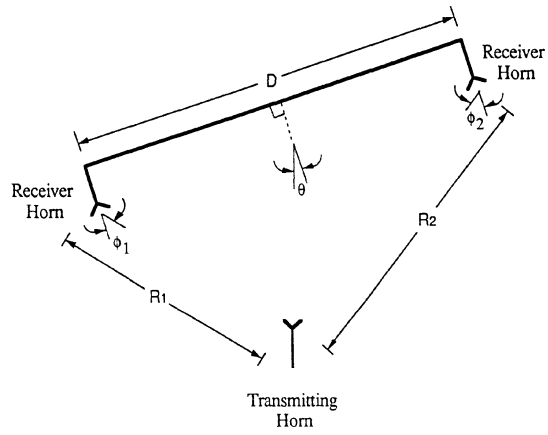

Fig. 4. Schematic diagram of geometry showing definitions of symbols.

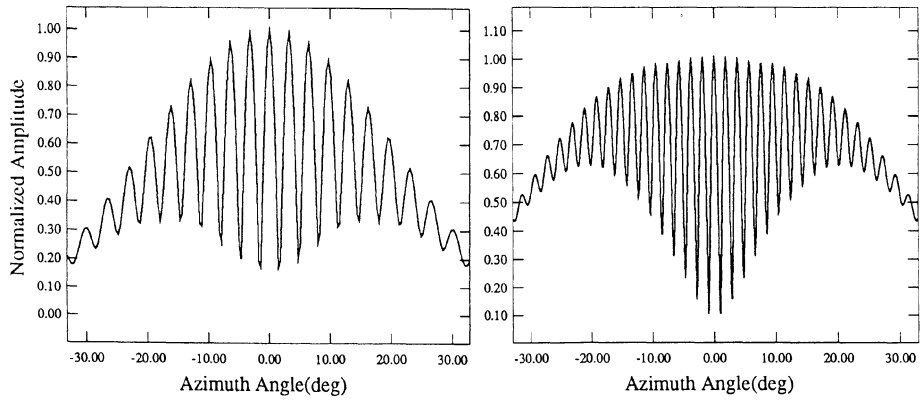

Fig. 5. Theoretical fringe patterns corresponding to experimental patterns in Fig. 2.

We can use equation (1) for resolution studies. We define angular resolution, $\Delta\theta$, as the angular width between adjacent nulls of the center fringe in the antenna pattern We define linear resolution Δx as $R(\Delta\theta)$. We performed a numerical study by calculating the fringe patterns for various antenna separations. From the fringe patterns we found the angular resolutions and then calculated the linear resolutions. We then made a sequence of plots of linear resolution vs. range for various ranges. Note that range is introduced in the calculation of the fringe pattern, and enters again in the linear resolution. Two of the results are shown in Figs. 7 and 8 for antenna separations of 0.7 m and 8 m. The conclusions obtained from these two extreme separations are applicable to all separations. We notice two main characteristics in the plots. The first is the linear portions of the curves in the right hand side of the plots. Following these curves from right to left we see that the curves start to level off. They truncate at the point where it becomes completely unfeasible to operate a physical array for the smaller ranges for the antenna separations given. A key point is that the limiting linear resolution is basically the same for any given antenna separation. The only way to improve the resolution beyond this point is to reduce the wavelength. In the figures shown the linear resolution limit is about 1.5 cm for a 3 cm wavelength when the beamwidth between first nulls is used as the measure of angular resolution. For high signal-to-noise ratios we can distinguish two objects as close as perhaps one tenth of the width between first nulls which gives a linear resolution limit of 1.5 mm. Regardless of the method for measuring resolution, once a method is chose, there is a clear limit to the linear resolution.

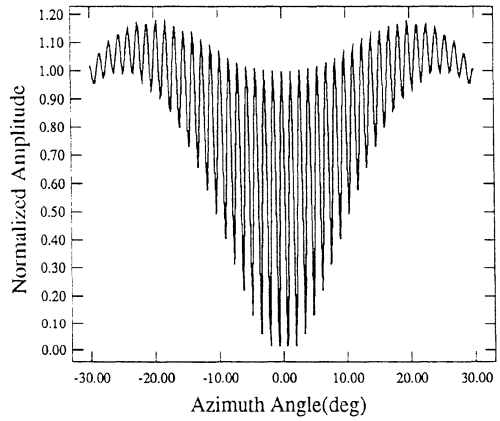

Fig. 6. Theoretical fringe pattern corresponding to experimental pattern in Fig. 3.

Another way to examine this limit is to observe the angular resolution. In Fig. 9 we show the same plot as in Fig. 7 but with an additional curve added for angular resolution (dotted line). The scale for it is shown on the right. Again we measure resolution as the angular separation between first nulls of the fringe pattern. In this figure we see that angular resolution stays nearly constant as we decrease the range (in the far field of the array), but with a further reduction in range (in the near field of the array) the beamwidth widens dramatically. The curve goes approximately as reciprocal distance. Hence, when we multiply angular resolution by the range for small values of range, we approach a constant value in the limit of small range.

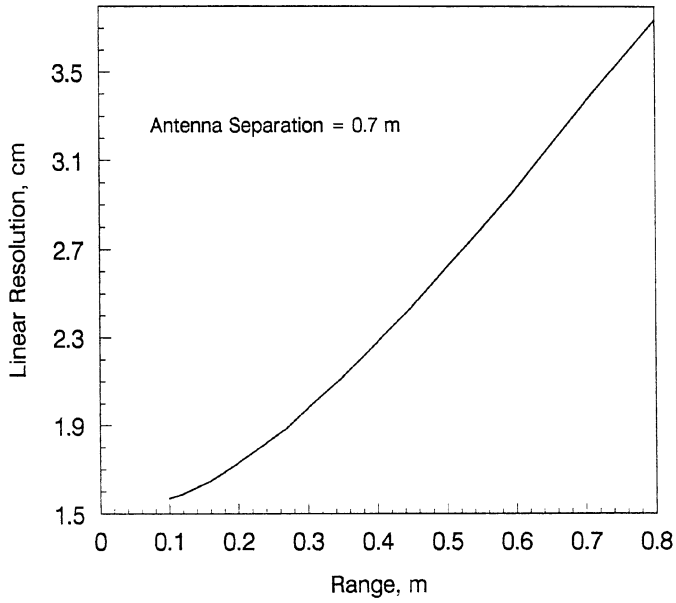

Fig. 7. Linear resolution vs. range for an antenna separation of 0.7 m.

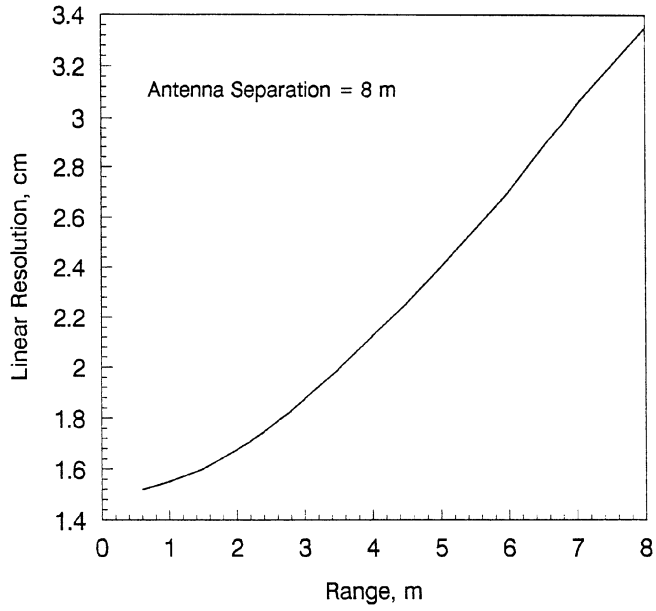

Fig. 8. Linear resolution vs. range for an antenna separation of 8 m.

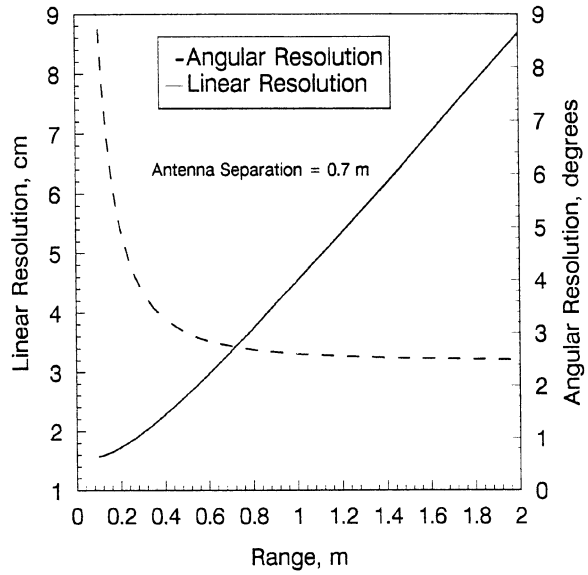

Fig. 9. Linear resolution (solid line) and angular resolution (dotted line) vs. range for an antenna separation of 0.7m. Note the extreme degradation of linear resolution as range decreases.

We can determine the theoretical resolution limit from equation (1) for small values of range. In the limit for $R<<R_1$ and $R<<R_2$, and small θ, $p(\phi_1)=p(\phi_2)=p(\phi)$. Then Eq. (1) becomes

$$f_r \approx \frac{p(\phi)}{R_1}\left[e^{-j2\pi(\frac{D}{2}+R\theta)/\lambda}+e^{-j2\pi(\frac{D}{2}-R\theta)/\lambda}\right]\approx\frac{2p(\phi)e^{-j\pi D/\lambda}}{R_1}\cos(2\pi R\theta/\lambda) \qquad (2)$$

where R_2 was set equal to R_1. At the first null of the fringe pattern $\theta_0=\lambda/4R$ so the beamwidth between first nulls, $\theta_{BWFN}=2\theta_0=\lambda/2R$. This is the limiting angular resolution using θ_{BWFN} as the measure of resolution. The limiting linear resolution is then $\theta_{BWFN}R=\lambda/2$which agrees with our numerical results (1.5 cm for λ=3 cm).

A global view of the resolution can be seen in Fig. 10 in which we have plotted range vs. antenna separation for a 3 cm wavelength with resolution as a parameter. The curves scale linearly with wavelength. Linear resolution has been selected as one-tenth of θ_{BWFN} to illustrate possible resolution under the best of conditions. Starting with 5 mm, we see that as resolution decreases the slope of the curve decreases. In other words, as we seek increasing resolution for a given range, we have to increase the antenna separation by a larger and larger amount. In the limit of small resolution the curve would become horizontal meaning that the antenna separation would go to infinity. This occurs around a limiting resolution of 1.5 mm as noted earlier for a measure of angular resolution being one-tenth the width between first nulls of the fringe pattern.

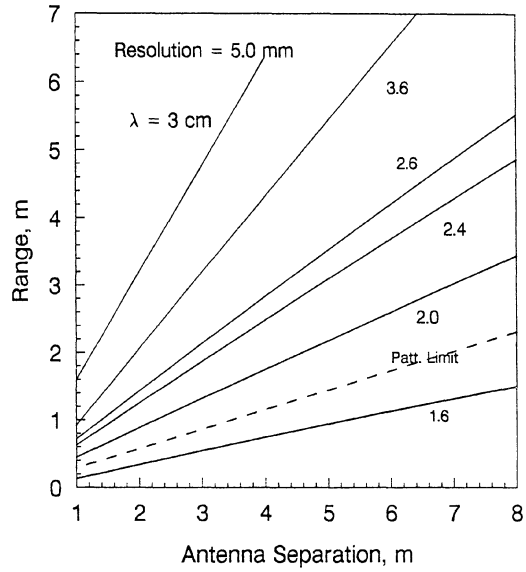

Fig. 10. Contours of constant resolution on a plot of range vs. antenna separation for a 3-cm wavelength. Resolution given is one-tenth of θ_{BWFN}.

A practical limit is imposed on the resolution curves. This is due to the beamwidth of the individual antennas in the array. The widest beamwidth occurs for an open ended waveguide. For this case the half-power beamwidth is about 60 degrees. As the range decreases the target (or transmitter in this case) moves out of the beamwidth of the receiving apertures. This imposes a limit on range as noted by the dotted line in Fig. 12. In a practical sense then, we could not achieve the theoretical resolution limit. (However, with difficulty we could use directional antennas and rotate these antennas as the range changes, but there would be little gain in resolution for this effort).

In conclusion, we see that for scanning antennas we achieve a limiting linear resolution caused by a combination of range, antenna separation, and wavelength. Theoretically, the limit is $\lambda/2$ using the beamwidth between first nulls of the central fringe as a measure of resolution. In laboratory situations we generally can achieve resolutions better than the beamwidth between first nulls because of a high signal-to-noise ratio. In the field the limit will be controlled by the physical situation governing the widest antenna separation, the shortest range, the highest usable frequency, the signal-to-noise ratio, and the beamwidth of the individual horns.

ACKNOWLEDGEMENT

The author thanks the Center for Nondestructive Evaluation at Iowa State University for support during this investigation.